COLLEGES OF NANOSCALE SCIENCE + ENGINEERING
SUNY POLYTECHNIC INSTITUTE

Quantum mechanical modeling of condensed matter systems

Samuel Skriloff, Steven Gassner, Sean Gibbons, Dr. Andrea Dziubek

Background

The Schrödinger Equation: 1D Lattice

Quantum mechanical systems are characterized by probabilistic states that are experimentally shown to have wavelike properties. As such, Erwin Schrödinger devised a **partial differential wave equation** describing the time evolution of a quantum system,

$$\boxed{\frac{\hbar^2}{2m}\nabla^2\Psi + V\Psi = i\hbar\partial_t\Psi}$$

where $\Psi = \Psi(\vec{r}, t)$ is a complex function called the **wavefunction** describing the quantum system. The constant $\hbar$ is the reduced Planck's constant, and m is the mass of the quantum object. For example, the wavefunction of an electron orbiting a single atom is a wave composed of spherical harmonics such that the **probability** of finding the electron at a position $\vec{r}$ is equal to the square modulus of the complex **amplitude** of the wave at that point, i.e. $|\Psi(\vec{r}, t)|^2$.

Applying separation of variables, (and focusing on only one dimension of space for simplicity) we find the very useful **time-independent Schrödinger Equation**,

$$\Psi(x,t) \equiv \psi(x)\cdot\varphi(t)$$

$$\boxed{\frac{\hbar^2}{2m}\psi'' + V\psi = E\psi}$$

where the separation constant E equals the **total energy** of the system. We can **discretize** space into a **one-dimensional lattice**, a set of N points $\{x_n\}_{n=1,\dots,N}$, spaced equally by a, with $\psi_n \equiv \psi(x_n)$, as follows,

$$\frac{\hbar^2}{2m}(\psi'')_n + V_n\psi_n = E\psi_n.$$

Applying the **finite element technique**, this turns into a tridiagonal matrix **eigenvalue equation**, (defining $t_0 \stackrel{\text{def}}{\equiv} \frac{\hbar^2}{2ma^2}$)

$$(\psi'')_n \approx \frac{\psi_{n-1} - 2\psi_n + \psi_{n+1}}{a^2}$$

$$\Rightarrow \quad -t_0\psi_{n-1} + (2t_0 + V_n)\psi_n - t_0\psi_{n+1} = E\psi_n$$

$$\begin{bmatrix} (2t_0+V_1) & -t_0 & & & -t_0 \\ \ddots & \ddots & \ddots & & \\ & -t_0 & (2t_0+V_n) & -t_0 & \\ & & \ddots & \ddots & \ddots \\ -t_0 & & & -t_0 & (2t_0+V_N) \end{bmatrix}\begin{bmatrix}\psi_1\\ \vdots\\ \psi_n\\ \vdots\\ \psi_N\end{bmatrix} = E\begin{bmatrix}\psi_1\\ \vdots\\ \psi_n\\ \vdots\\ \psi_N\end{bmatrix}$$

$$\hat{H}\psi = E\psi$$

where $\hat{H}$ is called the **Hamiltonian matrix**. It is an **operator** whose **observable** is the total energy of the system. In this simple case, the matrix takes a convenient tridiagonal form, but this in general does not always happen. It is the focus of this project to investigate numerical methods of exploiting physical symmetries in cases of a nontrivial Hamiltonian matrix to reduce it down to a form much more easily handled by computers.

Hamiltonian Construction using Green's Functions

Our technique for solving systems composed of semi infinite leads connected to a finite scattering model relies on the well known Green's equations:

$$\begin{cases} \mathbf{A}(E)\,\mathbf{G}^r(E) = \mathbf{I} \\ \mathbf{A}(E)\,\mathbf{G}^<(E) = \mathbf{\Sigma}^<(\mathbf{G}^r(E))^\dagger \\ \mathbf{A}(E)\,\mathbf{G}^>(E) = \mathbf{\Sigma}^>(\mathbf{G}^r(E))^\dagger \end{cases}$$

Where A is defined as $\mathbf{A} = E\mathbf{I} - \mathbf{H} - \mathbf{\Sigma}_L^r - \mathbf{\Sigma}_R^r - \mathbf{\Sigma}_{Phonon}^r$

Gr is called the retarded Green's function and describes the local density of states and the propagation of electrons injected in the device, and (Gr(E))† its Hermitian conjugate.
$\mathbf{G}^<(E)$, the lesser Green's function, represents the electron correlation function for energy level E. The diagonal elements of G<(E) represent the electron density per unit energy. G>(E), the greater Green's function, represents the hole correlation function for energy level E which is proportional to the density of unoccupied states. I is the identity matrix and H is the system Hamiltonian.
ΣrL and ΣrR represent the self-energies due to left and right contact coupling.

Our technique for constructing these green matrices for bounded scattering regions primarily employs the nested dissection algorithm. This allows for the constructions of an efficiently solvable sparse matrix as well as the ability to exploit existing symmetries for model reduction.

The technique starts by partitioning the lattice into two disconnected sets (L & R) and an interface (S).

With this partition the raw Hamiltonian can be written as the symmetric block matrix A:

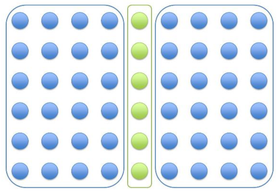

$$\text{With } \mathbf{A} = \begin{bmatrix} \mathbf{A}_{LL} & 0 & \mathbf{A}_{LS} \\ 0 & \mathbf{A}_{RR} & \mathbf{A}_{RS} \\ \mathbf{A}_{LS}^T & \mathbf{A}_{RS}^T & \mathbf{A}_{SS} \end{bmatrix}$$

$$\mathbf{A} = \underbrace{\begin{bmatrix} \mathbf{I} & 0 & 0 \\ 0 & \mathbf{I} & 0 \\ \mathbf{A}_{LS}^T\mathbf{A}_{LL}^{-1} & \mathbf{A}_{RS}^T\mathbf{A}_{RR}^{-1} & \mathbf{I} \end{bmatrix}}_{L} \underbrace{\begin{bmatrix} \mathbf{A}_{LL} & 0 & 0 \\ 0 & \mathbf{A}_{RR} & 0 \\ 0 & 0 & \widehat{\mathbf{A}}_{SS} \end{bmatrix}}_{D} \underbrace{\begin{bmatrix} \mathbf{I} & 0 & \mathbf{A}_{LL}^{-1}\mathbf{A}_{LS} \\ 0 & \mathbf{I} & \mathbf{A}_{RR}^{-1}\mathbf{A}_{RS} \\ 0 & 0 & \mathbf{I} \end{bmatrix}}_{L^{\mathrm{T}}}$$

Our G matrix becomes:

where $\widehat{\mathbf{A}}_{SS}$ is the Schur complement,

$$\widehat{\mathbf{A}}_{SS} = \mathbf{A}_{SS} - \mathbf{A}_{LS}^T\mathbf{A}_{LL}^{-1}\mathbf{A}_{LS} - \mathbf{A}_{RS}^T\mathbf{A}_{RR}^{-1}\mathbf{A}_{RS}.$$

$$\text{G} \quad \mathbf{G}^r = -\begin{bmatrix} \mathbf{A}_{LL}^{-1}\mathbf{A}_{LS}\mathbf{G}_{SL}^r & \mathbf{A}_{LL}^{-1}\mathbf{A}_{LS}\mathbf{G}_{SR}^r & \mathbf{A}_{LL}^{-1}\mathbf{A}_{LS}\mathbf{G}_{SS}^r \\ \mathbf{A}_{RR}^{-1}\mathbf{A}_{RS}\mathbf{G}_{SL}^r & \mathbf{A}_{RR}^{-1}\mathbf{A}_{RS}\mathbf{G}_{SR}^r & \mathbf{A}_{RR}^{-1}\mathbf{A}_{RS}\mathbf{G}_{SS}^r \\ 0 & 0 & 0 \end{bmatrix} + \begin{bmatrix} \mathbf{A}_{LL}^{-1} & 0 & 0 \\ 0 & \mathbf{A}_{RR}^{-1} & 0 \\ 0 & 0 & \widehat{\mathbf{A}}_{SS}^{-1} \end{bmatrix}\begin{bmatrix} \mathbf{I} & 0 & 0 \\ 0 & \mathbf{I} & 0 \\ -\mathbf{A}_{LS}^T\mathbf{A}_{LL}^{-1} & -\mathbf{A}_{RS}^T\mathbf{A}_{RR}^{-1} & \mathbf{I} \end{bmatrix}$$

Since G satisfies the relation: $\mathbf{G}^r = (\mathbf{I} - \mathbf{L}^T)\,\mathbf{G}^r + \mathbf{D}^{-1}\mathbf{L}^{-1}$

It decomposes as such:

$$\mathbf{G}_{SS}^r = \left(\widehat{\mathbf{A}}_{SS}\right)^{-1},$$
$$\mathbf{G}_{LS}^r = -\mathbf{A}_{LL}^{-1}\mathbf{A}_{LS}\mathbf{G}_{SS}^r,$$
$$\mathbf{G}_{RS}^r = -\mathbf{A}_{RR}^{-1}\mathbf{A}_{RS}\mathbf{G}_{SS}^r.$$

The diagonals describing L and R are computed independently from each other:

$$\mathbf{G}_{LL}^r = \mathbf{A}_{LL}^{-1} - \mathbf{A}_{LL}^{-1}\mathbf{A}_{LS}\left(\mathbf{G}_{LS}^r\right)^T = \mathbf{A}_{LL}^{-1} + \mathbf{A}_{LL}^{-1}\mathbf{A}_{LS}\mathbf{G}_{SS}^r\mathbf{A}_{LS}^T\mathbf{A}_{LL}^{-1}$$
$$\mathbf{G}_{RR}^r = \mathbf{A}_{RR}^{-1} - \mathbf{A}_{RR}^{-1}\mathbf{A}_{RS}\left(\mathbf{G}_{RS}^r\right)^T = \mathbf{A}_{RR}^{-1} + \mathbf{A}_{RR}^{-1}\mathbf{A}_{RS}\mathbf{G}_{SS}^r\mathbf{A}_{RS}^T\mathbf{A}_{RR}^{-1}$$

G< is calculated similarly and becomes:

$$\mathbf{G}_{SS}^< = \mathbf{G}_{SS}^r\left(\mathbf{\Sigma}_{SS}^<(\mathbf{G}_{SS}^r)^\dagger - \mathbf{A}_{LS}^T\mathbf{A}_{LL}^{-1}\mathbf{\Sigma}_{LL}^<(\mathbf{G}_{SL}^r)^\dagger - \mathbf{A}_{RS}^T\mathbf{A}_{RR}^{-1}\mathbf{\Sigma}_{RR}^<(\mathbf{G}_{SR}^r)^\dagger\right),$$
$$\mathbf{G}_{LS}^< = -\mathbf{A}_{LL}^{-1}\mathbf{A}_{LS}\mathbf{G}_{SS}^< + \mathbf{A}_{LL}^{-1}\mathbf{\Sigma}_{LL}^<(\mathbf{G}_{SL}^r)^\dagger,$$
$$\mathbf{G}_{RS}^< = -\mathbf{A}_{RR}^{-1}\mathbf{A}_{RS}\mathbf{G}_{SS}^< + \mathbf{A}_{RR}^{-1}\mathbf{\Sigma}_{RR}^<(\mathbf{G}_{SR}^r)^\dagger.$$

$$\mathbf{G}_{LL}^< = \mathbf{A}_{LL}^{-1}\mathbf{\Sigma}_{LL}^<(\mathbf{G}_{LL}^r)^\dagger - \mathbf{A}_{LL}^{-1}\mathbf{A}_{LS}(\mathbf{G}_{LS}^<)^\dagger$$
$$\mathbf{G}_{RR}^< = \mathbf{A}_{RR}^{-1}\mathbf{\Sigma}_{RR}^<(\mathbf{G}_{RR}^r)^\dagger - \mathbf{A}_{RR}^{-1}\mathbf{A}_{RS}(\mathbf{G}_{RS}^<)^\dagger$$

If needed, R and L are further split. A_{LL} and A_{RR} are decomposed by the same algorithm individually. G is calculated after A is fully reduced.

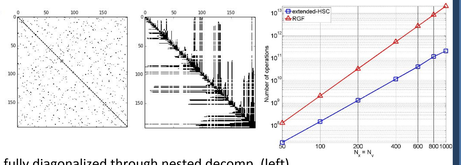

Figure 1. Before and after of matrix fully diagonalized through nested decomp. (left)
It preserves sparseness, produces G matrices and takes less operations than RGF (right)

Analytical Example: Graphene Band Structure

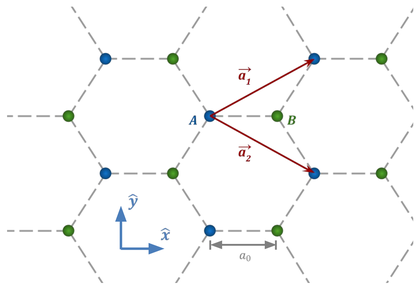

Figure 1. Graphene lattice. Sublattices are labeled A (blue) and B (green).

When a single layer of carbon atoms is isolated from graphite, it is called **graphene**. Graphene has been the subject of intensive study recently for its unique electrical properties, in particular for its electron band structure. Unlike many more complicated systems, the band structure for graphene can be solved analytically, and serves as a heuristic example for these more complicated cases where the aid of numerical techniques may be necessary.

Graphene forms a 2D hexagonal lattice, with a **two-atom basis**. This forms two **sublattices**, color-coded in Figure 1. Let us label them A and B. These sublattices lead us to relabel the components of our wavefunction, ψ, so that each component ψ_n has two parts: ψ_{nA} and ψ_{nB}. Stated otherwise,

$$\psi_n = \begin{bmatrix}\psi_{nA}\\ \psi_{nB}\end{bmatrix} \quad \Rightarrow \quad \psi = \begin{bmatrix}\psi_{1A}\\ \psi_{1B}\\ \psi_{2A}\\ \psi_{2B}\\ \vdots\\ \psi_{NA}\\ \psi_{NB}\end{bmatrix}$$

The time-independent Schrödinger equation, $\hat{H}\psi = E\psi$, for a **1D lattice** with a two-atom basis takes the form of a **block tridiagonal** matrix equation,

$$\begin{bmatrix} \begin{bmatrix}E_0 & -t_0\\ -t_0 & E_0\end{bmatrix} & \begin{bmatrix}0 & 0\\ -t_0 & 0\end{bmatrix} & & & \\ \begin{bmatrix}0 & -t_0\\ 0 & 0\end{bmatrix} & \begin{bmatrix}E_0 & -t_0\\ -t_0 & E_0\end{bmatrix} & \begin{bmatrix}0 & 0\\ -t_0 & 0\end{bmatrix} & & \\ & \begin{bmatrix}0 & -t_0\\ 0 & 0\end{bmatrix} & \begin{bmatrix}E_0 & -t_0\\ -t_0 & E_0\end{bmatrix} & \ddots & \\ & & \ddots & \ddots & \begin{bmatrix}0 & 0\\ -t_0 & 0\end{bmatrix} \\ & & & \begin{bmatrix}0 & -t_0\\ 0 & 0\end{bmatrix} & \begin{bmatrix}E_0 & 0\\ 0 & E_0\end{bmatrix} \end{bmatrix}\begin{bmatrix}\psi_{1A}\\ \psi_{1B}\\ \psi_{2A}\\ \psi_{2B}\\ \vdots\\ \psi_{(N-1)A}\\ \psi_{(N-1)B}\\ \psi_{NA}\\ \psi_{NB}\end{bmatrix} = E\begin{bmatrix}\psi_{1A}\\ \psi_{1B}\\ \psi_{2A}\\ \psi_{2B}\\ \vdots\\ \psi_{(N-1)A}\\ \psi_{(N-1)B}\\ \psi_{NA}\\ \psi_{NB}\end{bmatrix}$$

$$H_{n,n+1} \stackrel{\text{def}}{\equiv} \begin{bmatrix}0 & 0\\ -t_0 & 0\end{bmatrix}$$
$$H_{nn} \stackrel{\text{def}}{\equiv} \begin{bmatrix}E_0 & -t_0\\ -t_0 & E_0\end{bmatrix}$$
$$H_{n,n-1} \stackrel{\text{def}}{\equiv} \begin{bmatrix}0 & -t_0\\ 0 & 0\end{bmatrix}$$

which generalizes, since $\psi_n = \psi_0 e^{ikna}$, to the following summation of block matrices,

$$\sum_m H_{n,m}\psi_0 e^{i\vec{k}\cdot(\vec{r}_m - \vec{r}_n)} = E\psi_0$$

where $\vec{r}_n$ denotes the vector position of the n-th lattice site and $\vec{k}$ denotes the wavevector of the electron (proportional to its momentum).

In graphene, there is a total of 5 block matrices to consider (since every pair of A,B atoms has four neighboring pairs), and the summation becomes,

$$\left\{\begin{bmatrix}E_0 & -t_0\\ -t_0 & E_0\end{bmatrix} + \begin{bmatrix}0 & 0\\ -t_0 & 0\end{bmatrix}e^{i\vec{k}\cdot\vec{a}_1} + \begin{bmatrix}0 & 0\\ -t_0 & 0\end{bmatrix}e^{i\vec{k}\cdot\vec{a}_2} + \begin{bmatrix}0 & -t_0\\ 0 & 0\end{bmatrix}e^{-i\vec{k}\cdot\vec{a}_1} + \begin{bmatrix}0 & -t_0\\ 0 & 0\end{bmatrix}e^{-i\vec{k}\cdot\vec{a}_2}\right\}\psi_0 = E\psi_0$$

$$\Leftrightarrow \quad \begin{bmatrix} E_0 & -t_0\left(1 + e^{-i\vec{k}\cdot\vec{a}_1} + e^{-i\vec{k}\cdot\vec{a}_2}\right) \\ -t_0\left(1 + e^{i\vec{k}\cdot\vec{a}_1} + e^{i\vec{k}\cdot\vec{a}_2}\right) & E_0 \end{bmatrix}\psi_0 = E\psi_0$$

where $\vec{a}_1 = a_0\left(\frac{3}{2}\hat{\boldsymbol{x}} + \frac{\sqrt{3}}{2}\hat{\boldsymbol{y}}\right)$, $\vec{a}_2 = a_0\left(\frac{3}{2}\hat{\boldsymbol{x}} - \frac{\sqrt{3}}{2}\hat{\boldsymbol{y}}\right)$ (see Figure 1). Finally, solving this eigenvalue problem for E gives the **dispersion relation** (E vs. k graph) for electrons in graphene, given by the equation,

$$\boxed{E = \pm t_0\sqrt{1 + 4\cos\left(\frac{\sqrt{3}}{2}a_0k_x\right)\cos\left(\frac{3}{2}a_0k_y\right) + 4\cos^2\left(\frac{\sqrt{3}}{2}a_0k_x\right)}}$$

This represents the relationship between momentum and energy for conducting electrons in graphene.

A plot of this 2D dispersion relation (Figure 2) reveals six points around which the energy surfaces form a cone-like shape. These points are called **Dirac points**, and in the vicinity of these regions in k-space, electrons experience an energy-momentum relation similar to photons—that is, they act as if they are massless, and only travel at one speed regardless of energy.

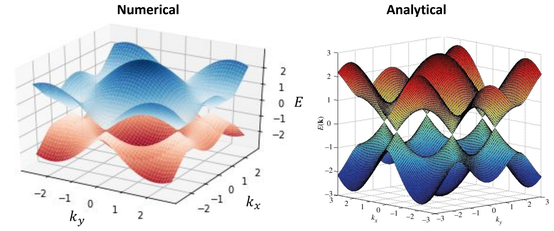

Figure 2. Graph of 2D dispersion relation for graphene computed numerically using our methods (left) and plotted using the analytically derived equation (right; source: Philosophical Transactions of the Royal Society A).

Numerical Analysis Techniques

Lancazo's Algorithm

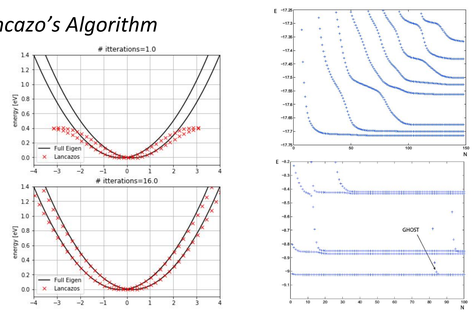

Figure 4. If only low eigenvalues are needed (often the case due to infinite low contribution, high energy states) Lancazo's algorithm can be employed to compute them significantly faster (convergence seen on bottom left took 1/80th the time as scipy solver) and with less memory requirements, as it does not iterate the matrix hamiltonian but rather uses it to create a tridiagonal "T" matrix with the same eigenvalues. Higher eigenvalues will converge after many iterations but loss of orthogonality can occur causing ghost eigenvalues to appear which converge to existing ones and increase its multiplicity. These limitations are seen in the right graphs. There are however heuristic techniques to check for ghosts.

Kernel Polynomial Method: Graphene Nanoribbon DOS

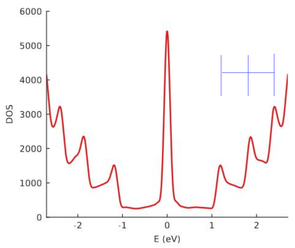

Figure 5. Density of states calculated for a 400x2 nm graphene nanoribbon using kernel polynomial method. Note the zero energy peak is does to zigzag edge states but the other peaks correspond very well to the predicted crossing of landau levels by the band structure quantized in the shorter direction (analytically predicted .603 eV energy step size in blue). Instead of computing the DOS at each site individually the total DOS is calculated with random weight for each site. Doing this multiple times and averaging together resolves the full DOS. Larger σ on random number generation more slowly produces smoother spectra. Larger system size also causes faster conversion.

Continuous ψ Approximation: Square Lattice vs. Graphene

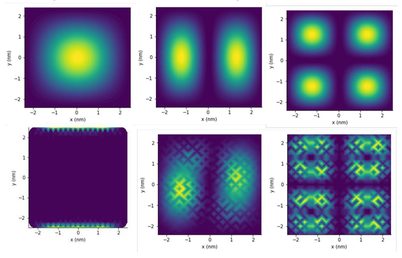

Figure 6. Site probability density functions ($\psi^*\psi$) for first, second, and third eigenstates (calculated by numpy sparse eigensolver) of the square well filled by square lattice (top) and graphene (bottom). Note that the first eigenstate in graphene is dominated by edge states and does not approximate vacuum ground state. The square lattice (because of it's cos dispersion relation approximating a vacuum's parabolic one) closely matches the analytically solvable quantized wavefunction in a square well, whereas graphene with it's Dirac points shows distortion. This discretization could be used to approximate the continuous Hamiltonian in unsolvable boundaries .

Conclusion

Research in condensed matter physics relies heavily on the ability to understand and simulate the quantum mechanical effects that give rise to material properties. These simulations usually involve a space-discretized form of the time-independent Schrödinger equation, giving rise to Hamiltonians in the form of excessively large sparse matrices.

Through the use of numerical techniques and the exploitation of physical symmetries, matrix Hamiltonians can be reduced to forms that are much more easily handled by computers, allowing for the calculation of material properties like band structure in cases where it is not analytically feasible.

Acknowledgments: Dr. Ji Ung Lee (SUNY Polytechnic Institute CNSE) whose lectures in NNSE 782 Topological Insulators: Dirac Condensed Matter Systems inspired much of this material.